

REVIEWS OF TOPICAL PROBLEMS

PACS numbers: 28.20.Pr, **61.05.–a**, 83.85.Hf

X-ray and neutron radiography and tomography in research and industry

A Yu Presnyakov, V I Mikerov, O A Gerasimchuk, D I Yurkov

DOI: https://doi.org/10.3367/UFNe.2023.11.039598

Contents

Abstract. **The state-of-the-art of the radiography and tomography using X-ray and neutron radiation is described. The methods are widely used in scientific research and industry due to the high penetrating power of radiation, different mechanisms of interaction with matter, the absence of sample destruction, and spatial resolution sufficient for a wide range of applications. Radiation methods are widely used in the nuclear fuel cycle, in studying the operation of fuel cells and materials under various conditions, in flaw detection, in biology, and in other fields of science and technology.**

Keywords: X-ray radiation, neutron radiation, radiography, tomography, neutron generators

1. Introduction

Radiography and tomography using X-ray and neutron radiation are among traditional methods of nondestructive testing and analysis of materials and various products. The main goals of using the methods are the quality control of manufactured articles in the process of their production, their technical diagnosis, flaw detection and control of the geometric characteristics of goods, scientific research, inspection of cargo, security checks of people and carry-on luggage, etc. The unique capabilities of the methods are used to develop technological processes, new products, and materials and to oversee the most crucial construction assemblies and mechanisms. The methods are also often used to check objects with defects that cannot be revealed visually and are applied to detect local imperfections in continuity, occlusions, differences in density, and deviations in the geometric structure.

Thanks to high penetrating power, the images obtained using X-ray and neutron radiography and tomography contain the most complete information about the internal structure of the studied objects.

This review discusses the application of the methods in the nuclear fuel cycle, in the study of electric cells, in checking the quality of turbine blades, in monitoring the operation of internal combustion engines, and in materials study. The issues of reverse engineering, space- and time-resolved radiography, and combined use of X-ray and neutron radiations are considered.

Readers interested in X-ray and neutron radiography and tomography can consult Refs [1–4] and the website of the International Society for Neutron Radiography [5].

A Yu Presnyakov [1,a], **V I Mikerov** [1,2,b], **O A Gerasimchuk** [1,c], **D I Yurkov** [1,2,d]
[1] Dukhov All-Russia Research Institute of Automatics (VNIIA), ul. Sushchevskaya 22, 127030 Moscow, Russian Federation
[2] National Research Nuclear University MEPhI (Moscow Engineering Physics Institute), Kashirskoe shosse 31, 115409 Moscow, Russian Federation
E-mail: [a] presnyakov_aleks@mail.ru, [b] vmikerov250846@yandex.ru, [c] oleg.gerasimchuk@bk.ru, [d] dmitry_yurkov@mail.ru

Received 6 July 2023, revised 17 November 2023
Uspekhi Fizicheskikh Nauk **194** (6) 618 – 629 (2024)
Translated by V L Derbov

2. Main areas of application

2.1 Nuclear fuel cycle

Present-day radiography and tomography allow checking the quality of parts, reveal the real condition of an exploited object, ensure the safety and reliability of the operation of nuclear power stations, and prevent possible accidents and catastrophes. Neutron and X-ray methods are mutually complementary tools used in the development and analysis of nuclear materials, etc.

The combined use of neutron and X-ray radiation in the nuclear fuel cycle is based on the substantial difference in their interaction with matter. Chemical elements with low electron density are poorly distinguished in X-ray radiographic images. On the contrary, the attenuation of neutrons by matter does not depend on its electron density. Thus, for example, hydrogen can be detected inside a metallic container, since the linear attenuation coefficient of thermal neutrons by hydrogen amounts to 3.44 cm^{-1}, and for Pb it equals 0.38 cm^{-1}.

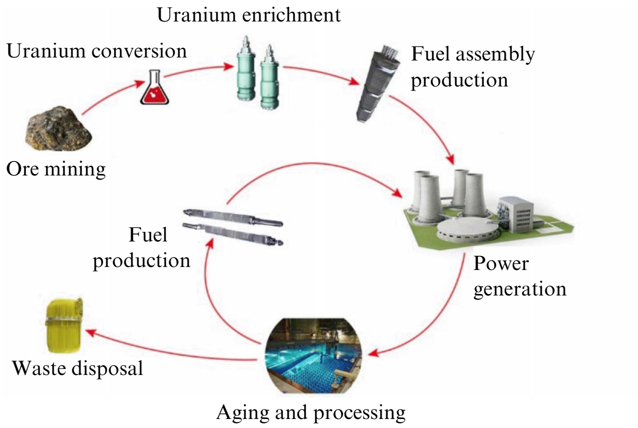

Figure 1. Main stages of nuclear fuel cycle [8].

Fission-fragment radiography (f-radiography) [6] is a unique method of analyzing radionuclides in the process of fission in a variety of rocks. It allows determining the quantitative content of fissile radionuclides, their spatial distribution, as well as the form in which they are present in the object of study. The method is instrumental, making it possible to perform analysis without chemical preparation or destruction of the sample and fixing the spatial location of thorium, uranium, plutonium, and other elements with high sensitivity. Fission-fragment radiography is based on the phenomenon of fission of nuclei of thorium, uranium, and plutonium in the field of thermal neutrons in a nuclear reactor and on the detection of fission fragments (tracks). Track detectors [7] fix the traces of fission fragments, which after appropriate processing are observed with an optical microscope.

The X-ray and neutron radiography application areas in the nuclear fuel cycle are (Fig. 1):

— study of composition and mineralogy of uranium ore;

— development and testing of fuel elements and materials;

— investigating the quality of welds;

— checking nuclear reactor vessels;

— handling nuclear waste.

2.1.1 Study of ore composition. Radiography and tomography are used as diagnostic tools for getting data on the geological volumetric composition of rock, in particular, core samples extracted from wells. Microcomputer X-ray tomography allows obtaining the results in an hour with a spatial resolution no worse than 6 μm and determining the content of gold, pyrite, zircon, and brannerite in various rocks. Uranite is found mainly in quartz matrices and carbon-containing components of rock in the form of round grains with a size of up to 200 μm [9].

Combining 2D and 3D X-ray imaging methods facilitates the understanding of the genesis of uranium-containing ores [10].

The use of X-ray diffraction in the study of ore rocks of the Malinovskoe uranium deposit revealed the presence of uranium in both authigenic and terrigenous components of the rocks; the presence of a finely dispersed 'mineral-free' form of uranium; and the participation of epigenetic processes at different times in the formation of deposit ores [11]. The sequence of formation and transformation of ores allows attributing them to a unique subtype of Mesozoic infiltration deposits from Western Siberia.

A combination of scanning electron microscopy and energy dispersive X-ray spectroscopy (SEM-EDS) offers an effective tool for determining uranium compounds. For this purpose, very thin sample plates are prepared and exposed to radiation in a nuclear reactor. The exposed samples produce tracks observed with a microscope. Images of the tracks determine the sample areas with increased uranium content, subsequently studied using SEM-EDS, the spectra of which are used to determine the mineralogy of the considered areas. As an example, we can present the studies carried out at the location of the former uranium factory in Grand Junction, Colorado, USA [12]. The results of studies by both methods have shown that the local uranium is coated by Al/Si gel and gypsum. The zones of smaller uranium content are filled with evaporite salts. The establishment of uranium mineralogy helps us to determine the rates of uranium release into underground waters.

2.1.2 Controlling enrichment of fuel rods. Natural uranium contains 99.284% of the U-238 isotope. The content of the U-235 isotope in natural uranium is only 0.711%. U-235 is the only isotope in nature present in substantial amounts and interacting with thermal neutrons. The distribution of uranium isotopes in a sample is determined by either radiography or gamma spectrometric measurements [13]. Historically, the first developed method of measuring enrichment was based on the fact that the intensity of gamma radiation from U-235 contained in sufficiently thick uranium samples is proportional to their enrichment [14]. As a rule, radiographic methods allow determining the distribution of microinhomogeneities over the surface and volume of a sample. Thermal neutron radiography yields the distribution of chemical elements such as Nd, Gd, and Pu in spent fuel rods [15]. The difference in absorption cross sections of U-235 and U-238 ensures nondestructive determination of the degree of fuel enrichment in fuel element pellets. The image contrast of the fuel element pellets with various densities depends on the energy of neutrons [16]. At energies above 19.7 meV, neutrons allow detection of pellets with minimum density. The rod itself is characterized by the maximum transmission. At a neutron energy of less than 6 meV, the pellets with the smallest density manifest themselves in the radiographic image as the darkest ones. The darker the image, the higher the enrichment.

2.1.3 Development and control of fuel elements. In Russia, the development of new kinds of fuel for nuclear power plants is in progress: the fuel for WWER-1000 and WWER-1200 reactors, the mixed fuel and fuel elements for floating power units [17]. Fuel behavior in the process of exploitation of fuel rods under extreme conditions, characterized by high energy release, temperature, pressure, and radiation, is being studied.

To get a license necessary to launch a nuclear reactor, it is checked, in particular, for safety in exploiting the fuel elements. The high sensitivity to the content of U-235 in radiographic studies when using slow neutrons is explained by their high penetration power in samples of natural uranium and different attenuation capacities of its isotopes. Neutron radiography methods allow studying the distribution of fissile material in fuel rods without compromising their integrity.

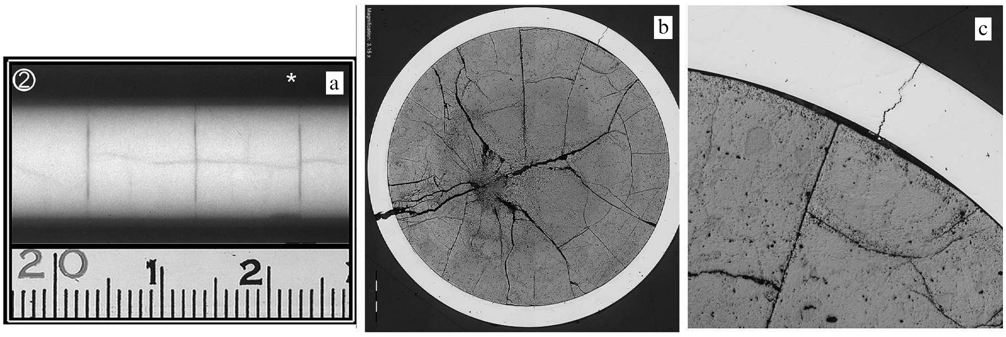

Figure 2. Neutron radiography image of a spent fuel element using thermal neutrons. Cracks (a) and voids (b) appear in the fuel. Fuel rod cladding is also prone to destruction (c) [20].

In contrast to neutron radiography, X-ray radiography is less used for the inspection of fuel rods, namely for the following reasons:

— uranium has a high attenuation coefficient for X-ray radiation (about 50 cm^{-1} for $E = 150$ keV);

— for thermal neutrons, the attenuation coefficient is 0.8 cm^{-1};

— in the case of thermal neutrons, U-235 and U-238 have substantially different attenuation capacities, which allows assessing the content of these isotopes;

— X-ray radiation does not allow detecting substances that strongly absorb thermal neutrons (boron, lithium, dysprosium, and gadolinium);

— X-ray radiation does not provide quantitative measurements of hydrogen content in the rod housing.

Nevertheless, X-ray radiography is used to control the manufacture of the claddings of heat-releasing elements that determine the reliability and safety of exploiting a nuclear power plant. To inspect them, a station for inspecting fuel rod welding joints [18] has been developed at the Design and Technology Institute of Scientific Instrument Engineering of the Siberian Branch of the Russian Academy of Sciences.

For decades, radiation radiography has been used to visualize fuel elements with two main purposes: verifying existing stocks and ensuring their quality. Review [19] presented the results of studying both intact and exposed assemblages consisting of various materials in various physical forms. Four decades of development have led to technologies through whose use it became possible to obtain 3D images of UO_2 granules 0.5 mm thick coated with an external layer.

Detecting the destruction of fuel contained in fuel rods (Fig. 2) is an important part of their study. Cracks (Fig. 2a) and voids (Fig. 2b) appear in the fuel. The claddings of fuel rods are also prone to destruction (Fig. 2c).

Zirconium alloys are the main material of fuel rod claddings in pressurized water and boiling water power reactors. Generally, the alloys contain hafnium, niobium, tin, iron, nickel, and chromium. Using zirconium is determined by a small coefficient of neutron capture. A radiographic study with thermal neutrons (Fig. 3) [21] shows that keeping the Zr(IV) alloy in water vapor for 8 hours at a temperature of 800 °C leads to inessential changes in it. When annealing the sample in the atmosphere with the addition of air, an increase in the changes is observed and a slight swelling of the sample occurs. When annealing in the atmosphere with the addition of nitrogen, significant swelling is observed with

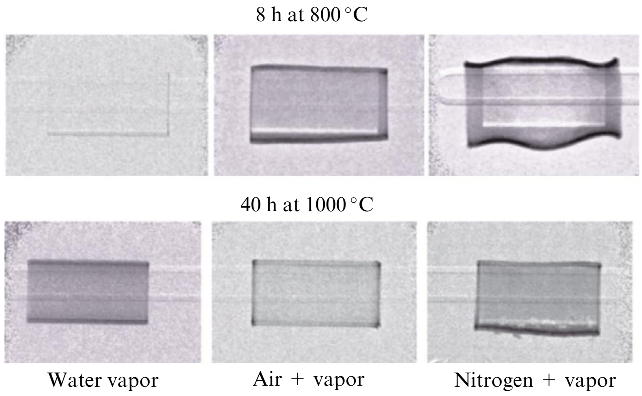

Figure 3. Neutron radiography images of a Zr(IV) sample placed in various atmospheres with a flow of water vapor (2 g h^{-1}) and nitrogen (10 l h^{-1}) [21].

a strong increase in the total cross section of interaction of thermal neutrons with the sample.

It is accepted that, in case of an accident with the cooling fluid, safety is guaranteed by the thermoplasticity of the fuel rod cladding. However, the oxygenation of the cladding made of zirconium by water vapor leads to the formation of free hydrogen:

$$Zr + 2H_2O = ZrO_2 + 4H\,. \tag{1}$$

If there are ruptures in the fuel element cladding, the hydrogen passes through them and is absorbed by metallic zirconium. The absorption of hydrogen by zirconium (Fig. 4) substantially deteriorates its plasticity [22]. In addition, the

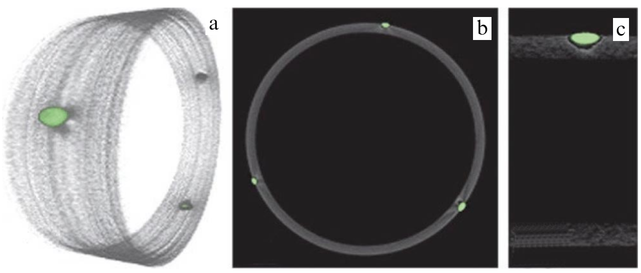

Figure 4. (a) Reconstructed 3D volume of a high-pressure pipe sample made of zircaloy (zirconium-tin alloy); (b, c) different sections of reconstructed volume [22].

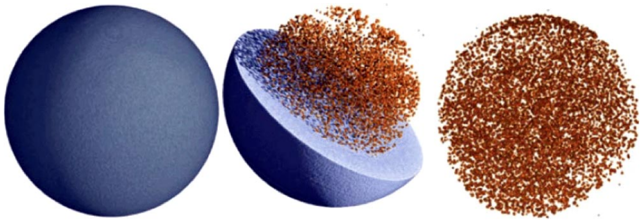

Figure 5. Image of a graphite sphere for a high-temperature reactor and results of measurements using neutron tomography [24].

oxygenation of zirconium leads to its becoming fragile. Thus, neutron radiography and tomography allow determining the hydrogen content in the cladding of the fuel element qualitatively and quantitatively with high sensitivity and accuracy.

The formation of hydrogen bubbles in high-pressure pipes made of zirconium alloys in nuclear reactors is one of the factors that limit trouble-free reactor operation [23]. The detection of the bubbles, determination of their dimensions, as well as the distribution of hydrogen in the surrounding matrix allow assessing the reactor lifetime. Neutron tomography is a means of studying the kinetics of hydrogen bubble formation.

A spherical fuel element intended for a high-temperature reactor is implemented in the form of a sphere 6 cm in diameter [24]. To study it, one of the methods is X-ray tomography, used to ensure the homogeneity of uranium dioxide particle arrangement in the carbon matrix and to develop a technological process, providing the central position of the particles in the matrix. As a result of X-ray tomographic analysis, the number of spatially separated fuel elements and their diameter were determined, which amounted to 8500 and 0.5 mm, respectively. Another result was the determination of the mean distance between fuel particles and the conformation of homogeneity of the fuel element filling. The result of X-ray studies of the spherical elements were confirmed by neutron tomography measurements (Fig. 5).

Monitoring spent fuel elements is a problem that arises in the development of new nuclear reactors. The problem consists in the high gamma activity of the fuel elements, which is an obstacle to using digital detectors and tomographic studies. This substantially increases the cost of the measurements. In Ref. [25], a low-power (250 kW) radiographic reactor with a relatively small neutron flux incident on the sample and a large signal-to-background ratio was used to examine fuel elements. An optical system was developed that allowed using a digital detector by placing it outside the neutron beam. The optical system consists of several coaxial nested Wolter mirrors and can operate with a polychromatic beam of thermal neutrons.

2.1.4 Handling nuclear waste. The radioactive waste classification has been proposed by the International Atomic Energy Agency (IAEA) [26]. The waste of low and medium activity is usually sealed in steel barrels, which are pressed, covered with concrete, and then placed in underground storage. Concrete is a porous material and transmits water. It is important to understand how this occurs during the storage of nuclear waste. Neutron radiography and tomography of concrete allow visualization of this process thanks to a high sensitivity of the neutron radiation to hydrogen. Neutrons allow measuring such physical properties of concrete as porosity, permeability, and sorbing capacity. The aim of the studies carried out in Refs [27, 28] was to improve the protective concrete constructions by decreasing the sorption of water and leaching of the concrete. The water sorption capacity of concrete depends on the initial water-to-cement ratio in the process of its production and the number of days that pass after its curing (Fig. 6). The smaller the amount of water used and the more time that has passed after the concrete curing, the lower its sorption capacity. In Fig. 6, the number of days passed after the concrete has cured is indicated at the bottom.

In atomic power engineering, concrete is used not only as a construction material but also as a material for biological protection. Concrete mix usually consists of cement, coarse and fine aggregate, water, and various additives. Studies of concrete properties were carried out using a setup placed at one of the horizontal channels of the VVR-K reactor [29]. Samples of three concrete grades were investigated. The distribution of pores and cracks in each sample was demonstrated. The difference in linear coefficients of neutron radiation attenuation by the samples did not exceed 10%. The rate of water migration in the concrete was assessed. One of the samples had a larger water penetration rate along the concrete height, which testifies to its higher porosity. The water migration rate along the height of this sample was 1.4 mm h^{-1}.

Neutron radiography methods were used to study the solidification processes in cement pastes used to build repositories or disposal sites of radioactive waste containing metallic aluminum. Various compositions of cement pastes with organic additives to suppress gas formation processes in the course of cement material curing were tested. The kinetics of cement paste curing were considered [30].

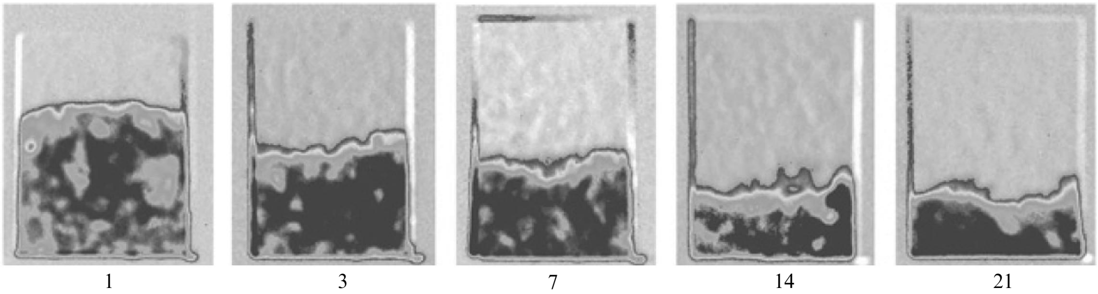

Figure 6. Neutron radiography images of a concrete sample after curing. Number of days after curing is indicated below images. The less water used and the more time that has passed since the concrete cured, the lower its sorption capacity [27, 28].

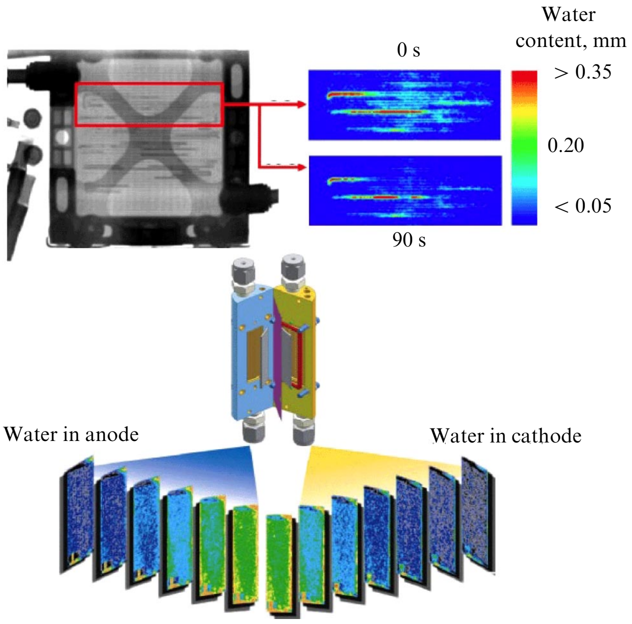

Figure 7. Neutron radiographic and tomographic images of a fuel cell with a polymer electrolyte membrane. Maximum distribution of water is observed in the anode of the cell [38].

The detection of radioactive materials is also of significance. For these aims, two approaches are used: an active one and a passive one. The active approach implies using a source of radiation and, in many cases, imaging the object of study [31–35]. Such an approach cannot be used in the immediate vicinity of humans and in noncontrolled zones of detection. The passive approach is related to using a system of detectors. In contrast to the active approach, it requires less equipment and is significantly cheaper to implement [36].

2.2 Electric cells

2.2.1 Evaluating water content. One of the important current applications of neutron and X-ray radiography is the study of fuel cells with a polymer electrolytic membrane. The cells can be applied in both stationary and mobile devices. Water plays an important role in the cells, particularly under low temperatures. On the one hand, liquid water is necessary in some amounts, since only a wet membrane transmits protons. On the other hand, the water content in gas-transporting channels and porous gas-diffusion layers strongly affects the density of the released energy and the lifetime of the materials used.

High-speed neutron tomography provides a quantitative analysis of water distribution in a cell and makes possible its computer simulation and creation of designs of the next generation [37]. The time dependence of water distribution in the cell anode and cathode, obtained by means of neutrons, is shown in Fig. 7 [38]. The horizontal lines on the left at the top are caused by liquid water moving along the channels intended for gas. On the right at the top, the distribution of water in the channels is shown immediately after their switching from hydrogen to deuterium gas and 90 s after the switching. It is seen that the water partially vanished in 90 s and was replaced by the practically transparent heavy water D_2O. At the bottom of the figure, the water distribution is shown as obtained from tomographic measurements of a test cell. Each slice in the figure has a thickness of 0.125 mm. The maximum water distribution is observed in the cell anode.

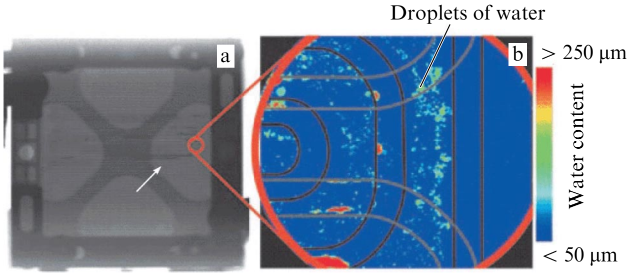

Figure 8. Images of an electrical element with polymer electrolyte membrane obtained using radiography with thermal neutrons (a) and synchrotron radiation (b). Arrow indicates area of hole drilling [39].

Combined use of neutron and X-ray radiography allows studying the distribution of liquid water in cells under realistic conditions of their exploitation. Neutrons easily penetrate through metallic walls, whereas X-ray radiation provides a high spatial (of the order of 1 μm) and temporal (at a level of 100 ms) resolution when using a synchrotron source (Fig. 8). Neutrons pass through metallic components of the cell, are sensitive to water and allow imaging of the entire cell. The necessity to drill holes in the face plates of the casing to pass the synchrotron radiation through them limits the field of view of the X-ray image, but at the same time provides visualization of water droplets a few microns in diameter [39]. The arrow in Fig. 8a indicates the region of the hole drilling.

2.2.2 Study of electric battery discharge. The images in Fig. 9 show tomograms of an alkaline electric battery using synchrotron and neutron radiation [39]. Images (a, c) were obtained before the discharge, and images (b, d), after it. The X-ray tomograms indicate considerable structural changes in the zinc powder (the particles in the center of the images), which were oxidated and partially dissolved in a KOH electrolyte. The cathode swelled and cracked because of a

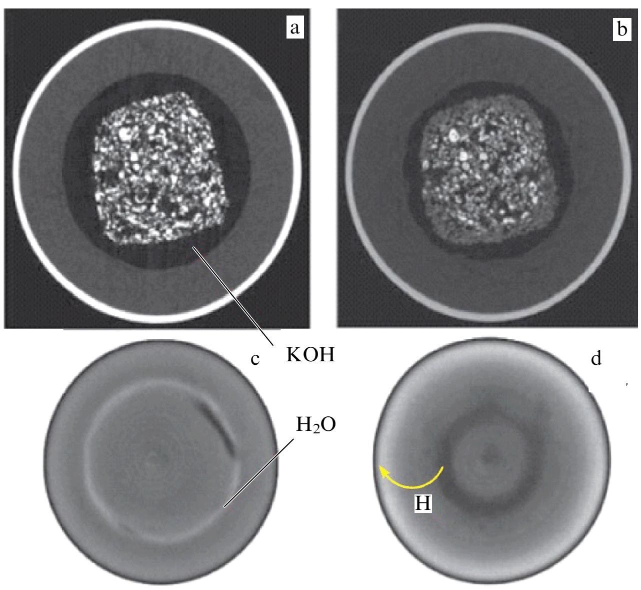

Figure 9. Tomograms of an alkaline cell: (a, b) in synchrotron radiation; (c, d) in neutron radiation [39].

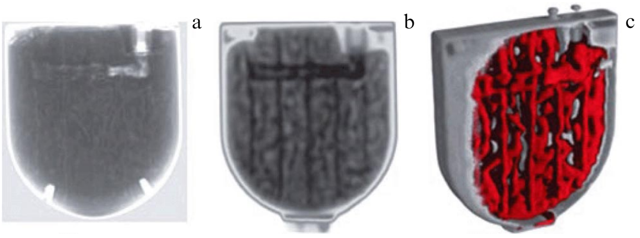

Figure 10. Radiographic and tomographic images of a lithium cell: (a) and (b) X-ray and neutron radiographic images; (c) neutron tomogram [39].

decrease in the amount of MnO_2 (the grey zone) and the penetration of hydrogen.

The complementary properties of X-ray and neutron radiation are well manifested in the study of lithium power cells. Since the cell contains solid LiI electrolyte, it demonstrates high reliability and is used, particularly, in medicine for heart pacemakers. It is important that the lithium cells work stably for a long time. The stability of operation depends on the change in the lithium distribution in the cell with time, the study of which allows optimizing cell operation and prolonging its lifetime. Thanks to a sufficiently large number of electrons in the shell of the atom, iodine is a high-contrast substance for X-ray radiation. At the same time, lithium strongly absorbs thermal neutrons. The X-ray image in Fig. 10a [39] mainly shows the iodine distribution in the cell. The neutron image in Fig. 10b demonstrates a distribution of lithium. The image in Fig. 10c is tomographic and shows a volume distribution of lithium. The cell size was 27 mm.

The processes that occur in vanadium cells depend on the physical and chemical properties of the surface of the materials used. To understand the influence of flow and formation dynamics of hydrogen bubbles, various type of cells were studied. The obtained data allow optimizing the cell design [40].

2.3 Other industrial products

2.3.1 Turbine blades. Turbine blades are used in gas turbine engines in aviation, shipbuilding, and power engineering. Issues concerning their production are some of the most science-intensive and complex. The blade is the most important part, taking on all the thermal load. The operation of the entire engine depends on its heat resistance. The blade working temperature is about 1000 °C. The gas temperature before the turbine is several hundred degrees Celsius higher than the melting point of the blade material itself. The uniqueness of the blade production technology consists in the casting, during which its directed crystallization occurs. The overhaul period of modern blades is about 1000 hours. The service life of PD-14 engine blades (aircraft turbofan engine of generation 5 and 5+) is 20,000 hours. The cost of aircraft engine blade production is comparable to that of a car. A blade is a virtually ideal single crystal with cavities inside for its cooling, usually with air, to prevent its melting at the operating temperature. The cavities are created by virtue of using ceramics, which is destroyed and removed through technological holes as the cavities are created. Neutron images of a blade without gadolinium ceramics and with it are shown in Fig. 11 [41]. When the ceramics contain gadolinium, their residuals in the blade cavities are detected by neutron radiography.

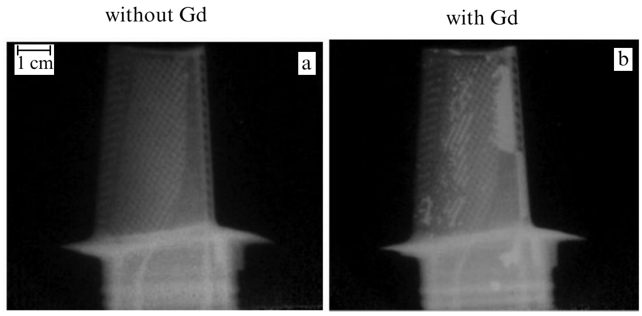

Figure 11. Neutron image of a turbine blade without (a) and with (b) gadolinium-containing ceramics [41].

2.3.2 Pyrotechnic devices. Pyrotechnic devices are critical components to carry a spacecraft into orbit. These devices are used for ignition, stage separation, satellite rotation, etc.

The French company Dassault Aviation develops and produces pyrotechnic components for the ARIANE 5 program. Before the launch, every pyrotechnic device is thoroughly tested. A total of about 800 various pyrotechnic devices are installed on ARIANE 5 [42–44]. The launch can be guaranteed under the condition of high quality of the installed devices. Neutron radiography using low-energy neutrons is a unique method of checking the condition of such devices and is widely used for these purposes.

The lack of explosives in a pyrotechnic device obviously leads to a failure in its operation. Reference [44] considers the possibility of using deuterium-tritium neutron generator together with a 12-bit CCD camera as a recorder to solve this problem. The studies revealed a typical change in the radiographic image intensity in different regions inside the metallic capsule with different wall thicknesses. The experiments have shown the difference between a material with a macroscopic absorption cross section of 13.9 b per molecule and aluminum having 1.62 b per molecule. There is a problem of detecting substances with close macroscopic absorption cross sections. It is established that, when using a neutron generator, it is possible to detect the difference between chalk powder and sucrose with attenuation coefficients of 0.13 cm^{-1} and 1.63 cm^{-1}, respectively.

X-ray tomography is also used to study pyrotechnic devices [45]. The images obtained when filling the device with calcium carbonate and epoxy compound significantly differ from those of unfilled samples. It was found that radiographic and tomographic X-ray images are characterized by good contrast. The possibility has been demonstrated of using X-ray tomographic measurements as an alternative tool for studying pyrotechnic devices when for some reason radiography cannot be performed.

2.3.3 Fuel injectors. Fuel injectors are also a target of nondestructive control. Images obtained in X-ray radiation at tube voltages of 100 kV and 190 kV, as well as in thermal neutrons, are shown in Fig. 12 [46]. The neutron radiograms are seen to reveal more details and in some sense to complete the X-ray images.

Microcomputer X-ray tomography demonstrates the effect of internal geometry of a fuel injector on the flow characteristics under realistic conditions [47]. A phase-contrast image can be used to study the internal cavitation and movement of a needle that, in this case, is a part of the fuel injector. The results of the study show that the flow

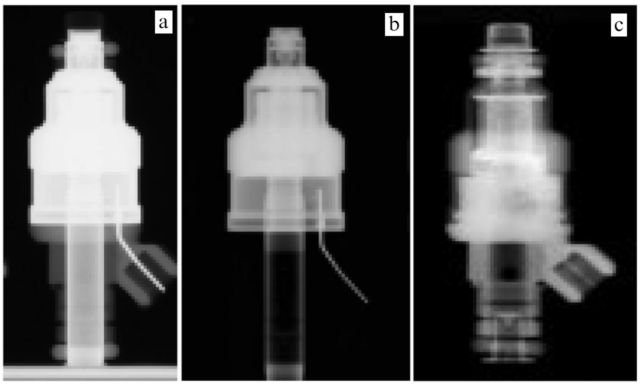

Figure 12. Fuel injector images. X-ray images at two tube voltages of 100 kV (a) and 190 kV (b). (c) Thermal neutron image [46].

characteristics are affected by the movement and excentric vibrations of the needle. X-ray imaging provides a good spatial and temporal resolution. Multiple exposures and absorption of X-ray radiation allow detecting the velocity and density distributions in the near field of the device.

Cavitation phenomena in fuel injectors were studied using neutron and X-ray radiation. The images have shown that the cavitation occurs in the injector nozzle [48–50]. From X-ray measurements, it follows that the cavitation volume has a substantial gradient with respect to the nozzle volume. The inner structure of the cavitation cloud is a hollow ball, formed at the nozzle entrance. The studies allowed developing a model of the injector nozzle geometry.

2.4 Dynamic radiography

The method of dynamic neutron radiography implements a nondestructive control of device operation in real time. The method is used when other kinds of radiation are inapplicable. A working internal combustion engine, whose operation can be observed due to the periodicity of the process and its synchronization with the operation of the neutron control system [51], can be considered an example. In Fig. 13, it is worth focusing attention on the position of the engine valves.

Neutron images of a burning cigarette were studied in the interests of a tobacco company [52]. The study allowed determining the change in the cigarette mass in the process of its burning, as well as the sedimentation, transmission, and evaporation of pyrolysis products. Additionally, the cigarette burning rate was determined.

In modern nuclear power production, matter is under the conditions of intense energy impact. This gives rise to a variety of complex hydrodynamic phenomena, the understanding of which is of interest for both applied and fundamental problems. The radiographic method using X-ray radiation offers new possibilities for the experimental study of a wide class of hydrodynamic, low-contrast, fast phenomena in plasma.

The X-ray method developed in Ref. [53] allows studying microobjects (including biological ones) with a spatial resolution of 10–20 μm and temporal resolution of 2–3 ns. This is important for understanding local dynamical problems and offers a key to using various collective phenomena.

In Ref. [54], X-ray radiography was used to study the development of Rayleigh–Taylor instability and pair shock-wave structures in nanosecond laser-induced plasma. The method is an upgrade of the technique of phase-contrast X-ray superhigh resolution radiography, which opens up new possibilities for the validation and development of theoretical models describing low-contrast phenomena in laser plasma, where a submicron accuracy of measurements is necessary.

In the case of neutrons, the studies are carried out at nuclear reactors. In this case, the degree of beam collimation and, therefore, the spatial resolution of the obtained images is worse. In Ref. [55], neutron radiography and tomography were used to clarify the liquid flow in rocks and the sorption of cadmium by them. Understanding these processes is necessary to predict the seismicity of a region, the phenomena of pollutant extrusion, the acceptability of underground storage of waste, the consumption of geothermal energy, and other issues. The different sensitivity of neutrons to isotopes of hydrogen has been exploited.

Understanding liquid flow in rocks is of crucial importance for the quantitative assay of many natural processes. Till recently, neutron methods were insufficiently used in geology because of the large amount of time needed for data acquisition. Reference [55] demonstrates the possibility of data acquisition in the case of leakage of a liquid and pollutants in rocks, in particular, of cadmium salts, which are present in many electronic devices, including power cells, and are a widespread pollutant of soil and ground water. The results of the study show that in porous rocks of centimeter scale the cadmium transfer occurs along the most favorable

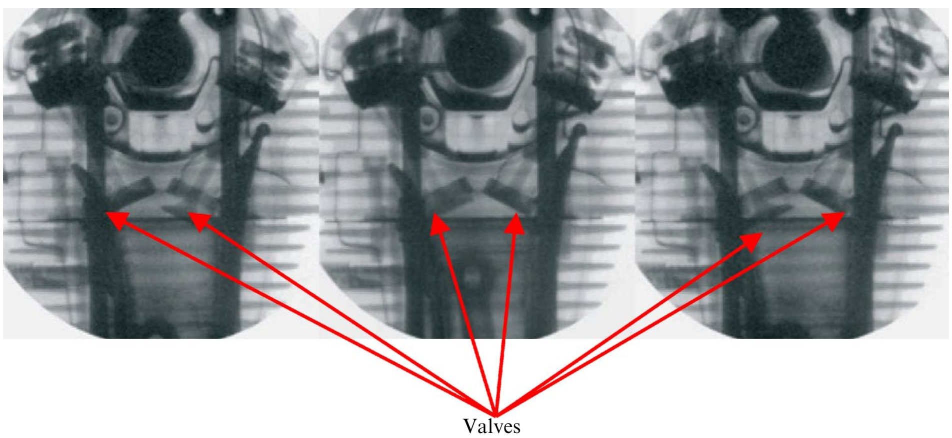

Figure 13. Study of operation of an internal combustion engine using dynamic neutron radiography [51].

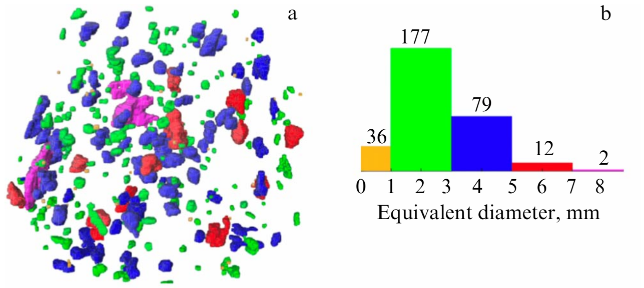

Figure 14. Spatial distribution (a) and diameter (b) of granite inclusions in a sample of lamprophyre [57].

paths. The neutron visualization of the process yields new information on the subsurface transfer of pollutants.

The study of biological phenomena is related to the dynamics of water penetration into plant roots. Reference [56] uses the contrast for thermal neutrons that exists for usual and heavy water. Gradual vanishing of the image in plant roots means the penetration of heavy water into them.

2.5 Materials study

Neutron tomography is one of the means to extract information on the spatial distribution and diameter of granite inclusions in lamprophyres (Fig. 14) [57], which are rare ultra-potassium magmatic rocks, mainly found in the form of dykes, lopoliths, laccoliths, stocks, and not large intrusions. They are alkaline undersaturated rocks with a high content of magnesium oxide, $> 3\%$, potassium oxide, sodium oxide, nickel, and chromium.

In the building industry, the composition of cured concrete and the mortar used is of importance. These data are, notably, required in cases where it is necessary to conclude whether the dosing of the components, first of all cement, corresponded to the specified grade of concrete. Such a necessity arises, for example, in cases of accidents or detecting insufficient concrete strength. The neutron radiography and tomography used to determine the composition of the cured concrete are of significant interest both for building companies directly responsible for the concrete quality and for the inspection bodies (courts, etc.). The study of cured concrete by neutron imaging is a useful tool in the study of the causes of its cracking and appearance of defects (Fig. 15) [58].

The reconstruction of tomograms is often performed using the Octopus program [59], and, for the analysis of sample porosity, the VGStudio package [60] is used.

Due to the large cross section of interaction of thermal neutrons with hydrogen, neutron tomography is sensitive to its content and is often used to detect hydrogen-containing substances and to complement X-ray measurements. An example is $AlSi_6Cu_4$ aluminum foam, in the production of which at the first stage the foaming agent TiH_2 is used. Its distribution before and after the foaming process is of great importance for the entire process and determines the foam quality (Fig. 16) [61].

In the neutron tomogram (Fig. 16b), TiH_2 agglomerates are shown in red. When studying the TiH_2 distribution, X-ray tomography provides necessary spatial resolution, whereas neutron tomography allows detecting TiH_2 agglomerates.

Reference [62] discusses the necessity of using neutron radiography in the study of diffusion processes and the kinetics of chemical reactions. As an example, the zirconium

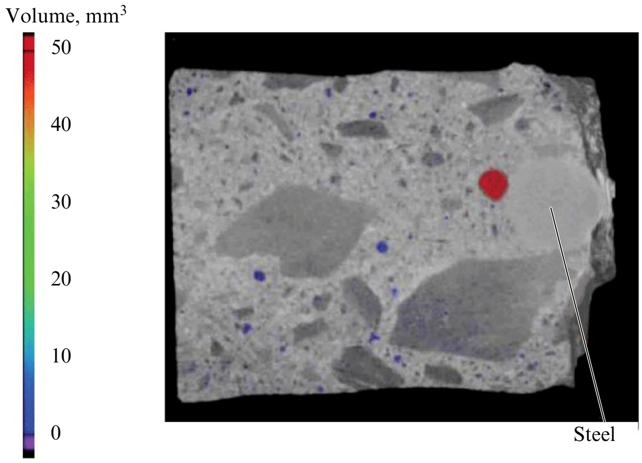

Figure 15. Tomogram used to analyze concrete porosity [58].

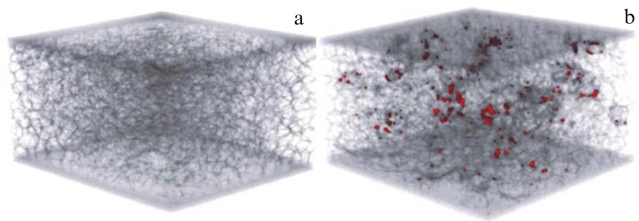

Figure 16. X-ray (a) and neutron (b) tomograms of $AlSi_6Cu_4$ foam. Agglomerates of TiH_2 are shown in red in neutron tomogram [61].

alloy is used, where the diffusion of hydrogen, its absorption upon high-temperature oxidation, and reactions occurring in the atmosphere of nitrogen and air are explored. The advantages of using neutron radiography are being discussed.

Using neutron and X-ray radiation, the behavior of water in a steel pipe was studied [63]. The results of the simulation performed in this paper show the possibility of measuring the hydrogen density under high pressure in metallic vessels.

3. Reverse engineering

Reverse engineering is a process of creating a 3D model of the product under study, writing the design documentation, and making the product itself [64].

Reverse engineering is applied when

— the design documentation is absent or has to be restored;

— the present documentation is irrelevant;

— the characteristics of the existing product have to be improved;

— a new product is to be developed.

Till recently, it was believed that the reverse engineering requires a long time, is costly, and suffers from many limitations. However, the appearance of advanced computer tools for determining a subject's characteristics, imaging, and processing software changed this point of view. Usually, the data for reverse engineering of products are obtained using an optical or laser 3D scanner, which provides information on the exterior geometry of the product. An advantage of using neutron tomography consists in the determination of the dimensions of internal structures without their physical destruction should the sample contain material of low-contrast or impermeable for X-rays.

Neutron tomograms are usually obtained at reactors, using cold, thermal, epithermal, and fast neutrons. The obtained set of 3D data contains information on the local distribution of the radiation attenuation coefficient in a sample. The sample boundaries are determined by the gradient between the adjacent voxels (elements of volume image, containing values of the mapped quantity). The data are converted into a geometric model by means of a triangle mesh, connecting adjacent elements and forming a set of triangles, describing the real surface. This procedure also describes voids and inhomogeneities.

In Ref. [65], neutron tomograms were used for reverse engineering of gas turbine components. Naturally, of importance is the position of the sample on the rotary stage and the exposure time. The reconstruction of the sample structure is to be performed using the appropriate software. For inhomogeneous samples, it is reasonable to export and process the tomograms of the constituent parts individually.

X-ray radiation is used, particularly in the reverse engineering of printed-circuit boards [66].

4. Neutron generators in radiography

Fast neutrons are used when it is necessary to image products having low transparency for thermal neutrons and containing substances with low contrast for these neutrons. The sources of fast neutrons are nuclear reactors, accelerators, and neutron generators. Portable neutron generators allow designing equipment that can work in laboratory and field conditions. A promising area of developing such equipment is the use of generators implementing the method of accompanying particles (Fig. 17) [67, 68]. These generators emit neutrons with an energy of 14 MeV as a result of the nuclear reaction

$$d + t \rightarrow \alpha + n\,. \tag{2}$$

The alpha particle escapes together with the neutron virtually in the opposite direction. Therefore, the detector of alpha particles detects the escape direction of the neutron. Such is the ING-27 generator (Dukhov All-Russia Research Institute of Automatics), with an output of 1×10^8 neutrons/s in the stationary mode of operation, the neutron energy being 14 MeV [70], or the API 120 generator (Thermo Scientific) [71] with an output of 2×10^7 neutrons/s.

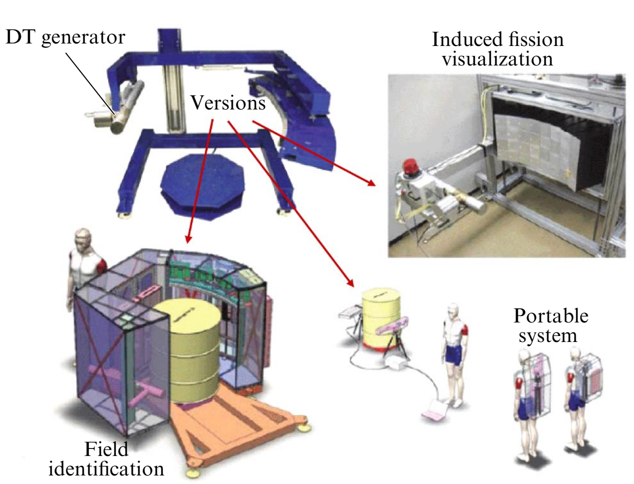

Figure 17. Oak Ridge National Laboratory setup with neutron generator using method of accompanying particles [69].

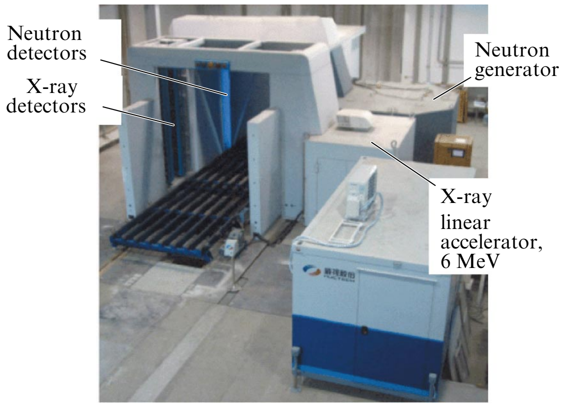

Figure 18. Photograph of stereoscopic setup for luggage inspection using two kinds of radiation, produced by CSIRO (Australia) and Nuctech Company Limited (China) [71].

The authors of Ref. [71] proposed a mobile system of luggage inspection based on using X-ray radiation and a generator of fast neutrons. For cargo inspection, the system implies using a tunnel 1.1 m in size, an X-ray generator with a tube voltage of 170 kV, and a DD generator of 2.5-MeV neutrons (Fig. 18). The sources of X-ray and neutron radiations are located at the bottom of the setup.

5. Conclusion

The review covers the main applications of neutron and X-ray radiography and tomography in research and industry. The methods considered have their limitations, associated with the use of ionizing radiation and the necessity of radiation protection. X-ray and neutron radiation is used first of all for revealing defects that cannot be detected with the naked eye. They are efficient due to the high penetration power of the radiation, different mechanisms of interaction with matter, the absence of sample destruction, and a spatial resolution sufficient for a wide range of industrial applications. The radiation can pass through various materials, so it is applicable for inspecting objects and materials without the necessity to move them. The methods are mainly used to test products in the nuclear fuel cycle, to study the behavior of materials under various conditions, to transport of substances in fuel cells, to detect flaws in various products, and for biological studies.

The issues excluded from consideration in the present review include, in particular, the methods of X-ray and neutron radiography and tomography in different beams using phase contrast. In the review, we do not consider experimental setups used for their implementation and do not comment on the advantages of joint application of both kinds of radiation. The choice of materials for the review, nevertheless, seems justified. It acquaints the reader with the state-of-the-art of X-ray and neutron radiography and tomography and is useful as an introduction to radiation methods of research.

There are a considerable number of areas where proceeding to digital methods is profitable due to saving time and labor, eliminating expenditures for film, chemicals, and their utilization, and increasing production efficiency. In this case, the reduction of measuring time is ensured by the automated positioning of the products and saving the obtained images in seconds.

Progress with the methods of digital radiography and tomography at present is related mainly to the development and improvement of research methods, sources and recorders of radiation, high-efficiency algorithms and software, as well as the automation of measurements.

References

1. Tyufyakov N D, Shtan' A S *Osnovy Neitronnoi Radiografii* (Fundamentals of Neutron Radiography) (Moscow: Atomizdat, 1975)
2. Gurvich A M *Fizicheskie Osnovy Radiatsionnogo Kontrolya i Diagnostiki* (Physical Foundations of Radiation Monitoring and Diagnostics) (Moscow: Energoatomizdat, 1989)
3. Kalender W *Computed Tomography: Assessment Criteria, CT System Technology, Clinical Applications* (Chichester: Wiley, 1986); Translated into Russian: *Komp'yuternaya Tomografiya: Osnovy, Tekhnika, Kachestvo Izobrazhenii i Oblasti Klinicheskogo Ispol'zovaniya* (World of Biology and Medicine, III, 03) (Moscow: Tekhnosfera, 2006)
4. Pizzutiello R J (Jr.), Cullinan J E *Introduction to Medical Radiographic Imaging* (Rochester, NY: Health Sciences Division, Eastman Kodak Co., 1996)
5. Intern. Society for Neutron Radiography, https://www.isnr.de
6. Rybin I V "Radiograficheskie metody" ("Radiographic methods"), presentation, https://thepresentation.ru/fizika/radiograficheskie-metody
7. Rikhvanov L P, Zamyatina Yu L, Arkhangel'skaya T A *Izv. Tomsk. Politekh. Univ.* **311** (1) 123 (2007)
8. "Yadernoe toplivo: ot rudy do utilizatsii." Nauchno-delovoi Portal "Atomnaya Energiya 2.0." Nauchno-delovoi Portal "Atomnaya Energiya 2.0" ("Nuclear fuel: from ore to utilization." Scientific and Business Portal "Atomic Energy 2.0"), https://www.atomic-energy.ru/SMI/2017/03/15/73650
9. De Beer F C *J. South. Afr. Inst. Min. Metall.* **115** 913 (2015)
10. Sebola P "Characterisation of uranium-mineral-bearing samples in the Vaal Reef of the Klerksdorp Goldfield, Witwatersrand basin", Master Science Thesis (Johannesburg: Faculty of Science, Univ. of the Witwatersrand, 2014); http://hdl.handle.net/10539/16820
11. Kondrat'eva I A, Maksimova I G, Nad"yarnykh G I *Lithology Mineral Resources* **39** 333 (2004); *Litologiya Poleznye Iskopaemye* (4) 387 (2004)
12. Johnson R H, Hall S M, Tigar A D *Geosciences* **11** 294 (2021)
13. Chirilă C C, Ha T M H *Commun. Comput. Phys.* **21** 1475 (2017)
14. Bushuev A V *Metody Izmereniya Yadernykh Materialov* (Methods of Measuring Nuclear Materials) (Moscow: MIFI, 2007) Textbook for Students of Higher Educational Institutions
15. Barmakov Yu N et al. *Yad. Fiz. Inzhiniring* **1** (1) 61 (2010)
16. Tremsin A S et al. *J. Nucl. Mater.* **440** 633 (2013)
17. Troyanov V M et al. "Razrabotka novykh vidov topliva i konstruktsionnykh materialov dlya krupnomasshtabnoi yaderno-energeticheskoi sistemy Rossii (Rossiya, Moskva, 26–27.05.2010)" ("Development of new types of fuel and structural materials for a large-scale nuclear energy system of Russia (Russia, Moscow, 26–27.05.2010)", http://www.myshared.ru/slide/308297
18. Vorob'ev V V et al. *Datchiki Sistemy* (2) 6 (1999)
19. Parker H M O'D, Joyce M J *Prog. Nucl. Energy* **85** 297 (2015)
20. Jenssen H K et al. *Prog. Nucl. Energy* **72** 55 (2014)
21. Grosse M, Schillinger B, Kaestner A *Appl. Sci.* **11** 5775 (2021)
22. Agrawal A et al. *J. Nucl. Mater.* **421** 47 (2012)
23. Bobkov G O *Politekh. Molodezh. Zh.* (07) 1 (2020) http://dx.doi.org/10.18698/2541-8009-2020-7-629
24. Lehmann E H, Vontobel P, Hermann A *Nucl. Instrum. Meth. Phys. Res. A* **515** 745 (2003)
25. Rai D K et al. *Nucl. Instrum. Meth. Phys. Res. A* **879** 141 (2018)
26. Normy MAGATE po bezopasnosti dlya zashchity lyudei i okhrany okruzhayushchei sredy. Klassifikatsiya radioaktivnykh otkhodov. Rukovodstvo po bezopasnosti GSG-1 (IAEA Safety Standards for the Protection of People and the Environment. Classification of Radioactive Waste. Safety Guide No. GSG-1) (Vienna: IAEA. International Atomic Energy Agency, 2014); https://www.iaea.org/ru/publications/10534/klassifikaciya-radioaktivnyh-othodov
27. De Beer F C, Strydom W J, Griesel E J *Appl. Radiat. Isotopes* **61** 617 (2004)
28. De Beer F C, le Roux J J, Kearsley E P *Nucl. Instrum. Meth. Phys. Res. A* **542** 226 (2005)
29. Dyusambaev D S et al. "Nerazrushayushchie issledovaniya vnutrennei struktury betona raznykh marok" ("Non-destructive studies of the internal structure of concrete of different grades") *Recent Contributions Phys.* (1(80)) 48 (2022) https://doi.org/10.26577/rcph.2022.v80.i1.06
30. Kichanov S E et al. *Phys. Part. Nucl. Lett.* **17** 73 (2020); *Pis'ma Fiz. Elem. Chastits At. Yadra* **17** 63 (2020)
31. Gozani T *Active Nondestructive Assay of Nuclear Materials: Principles and Applications* (Washington, DC: The Commission. GPO Sales Program, U.S. Nuclear Regulatory Commission, 1981)
32. Singh M *Med. Phys.* **10** 421 (1983)
33. Runkle R C, Chichester D L, Thompson S J *Nucl. Instrum. Meth. Phys. Res. A* **663** 75 (2012)
34. Norman D R et al. "Active nuclear material detection and imaging", in *Proc. of the 2005 IEEE Nuclear Science Symp. Conf. Record, Fajardo, Puerto Rico, USA 23–29 October 2005* (Piscataway, NJ: IEEE, 2005) p. 1004, https://doi.org/10.1109/NSSMIC.2005.1596423
35. Jones J L et al. *Nucl. Instrum. Meth. Phys. Res. A* **562** 1085 (2006)
36. *Safeguards Techniques and Equipment* (Intern. Nuclear Verification Ser., 1020-6205, No.1, Rev. 2) 2011 ed. (Vienna: Intern. Atomic Energy Agency, 2011); https://www.iaea.org/publications/8695/safeguards-techniques-and-equipment
37. Ziesche R F et al. *Nat. Commun.* **13** 1616 (2022)
38. Kardjilov N et al. *Mater. Today* **14** (6) 248 (2011) https://doi.org/10.1016/S1369-7021(11)70139-0
39. Banhart J et al. *Int. J. Mater. Res.* **101** 1069 (2010)
40. Eifert L et al. *ChemSusChem* **13** 3154 (2020)
41. Yu Y et al. *Appl. Sci.* **11** 6050 (2021)
42. Bayon G *Nucl. Instrum. Meth. Phys. Res. A* **424** 92 (1999)
43. Raghu N et al. *AIP Conf. Proc.* **989** 202 (2008)
44. Namboodiri G N et al. *J. Nondestruct. Eval.* **39** 16 (2020)
45. Namboodiri G N et al. *Eur. Phys. J. Plus* **136** 945 (2021)
46. Imaging. Neutron and X-ray images produced in Phoenix's neutron imaging center, https://www.phoenixneutronimaging.com/insights-and-updates/neutron-image-gallery
47. Wu Z et al. *Automot. Innov.* **2** 79 (2019)
48. Takenaka N et al. "Application of neutron radiography for visualization of cavitation phenomena in a fuel injection nozzle of a diesel engine", in *Proc. of the 10th Intern. Conf. on Liquid Atomization and Spray Systems, ICLASS-2006, August 27 – September 1, 2006, Kyoto, Japan* (Ed. H G Fujimoto) paper ID ICLASS06-174
49. Mitroglou N et al. *Exp. Fluids* **57** 175 (2016)
50. Matusik K E et al. *Int. J. Engine Res.* **19** 963 (2018)
51. Brunner J et al. "Dynamic neutron radiography of a combustion engine", in *16th World Conf. on Nondestructive Testing, NDT, August 30 – September 3, 2004, Montreal, Canada* (Montreal, QC: Canadian Institute for ND, 2004); https://www.ndt.net/article/wcndt2004/pdf/radiography/366_brunner.pdf
52. Brenizer J S et al. *Beiträge Tabakforschung Int.* **17** (1) 3 (1996) https://doi.org/10.2478/cttr-2013-0648
53. Zhigalin A S et al. "Prostranstvennye i vremennye kharakteristiki izlucheniya kompaktnogo rentgenovskogo radiografa na osnove vakuumnogo dugovogo razryada" ("Spatial and temporal characteristics of radiation of a compact X-ray radiograph based on a vacuum arc discharge"), in *Vzaimodeistvie Izluchenii s Tverdym Telom, VITT 2017, Materialy 12-i Mezhdunarodnoi Konf., Minsk, Belarus, 19–22 Sentyabrya 2017 g.* (Interaction of Radiation with a Solid Body, VITT 2017, Proc. of the 12th Intern. Conf., Minsk, Belarus, September 19–22, 2017) (Exec. Ed. V V Uglov) (Minsk: Izd. Tsentr BGU, 2017) p. 449; https://elib.bsu.by/handle/123456789/182299

54. Makarov S S ''Izuchenie ekstremal'nykh gidrodinamicheskikh yavlenii v lazernoi plazme metodom kogerentnoi rentgenovskoi radiografii sverkhvysokogo razresheniya'' (''Study of extreme hydrodynamic phenomena in laser plasma by the method of coherent X-ray radiography of ultra-high resolution''), Abstract of the PhD Thesis for the degree of candidate of phys. and math. sciences (Moscow: Joint Institute for High Temperatures, Russian Academy of Sciences, 2022)
55. Cordonnier B et al. *Front. Earth Sci.* **7** 306 (2019)
56. Tötzke C et al. *Sci. Rep.* **7** 6192 (2017)
57. Zel I et al. *J. Imaging* **8** (3) 80 (2022)
58. Garbe U et al. *Phys. Procedia* **88** 13 (2017)
59. Dierick M, Masschaele B, Van Hoorebeke L *Meas. Sci. Technol.* **15** 1366 (2004)
60. VGStudio MAX, https://www.volumegraphics.com/en/products/vgsm.html
61. Solórzano E et al. *Nucl. Instrum. Meth. Phys. Res. B* **324** 29 (2014)
62. Grosse M, Schillinger B, Kaestner A *Appl. Sci.* **11** 5775 (2021)
63. Wei T et al. *AIP Adv.* **12** 045220 (2022)
64. ''Primenenie komp'yuternoi tomografii dlya obratnogo proektirovaniya izdelii'' (''Application of computed tomography for reverse engineering of products''), https://sovtest-ndt.ru/reverseeng/
65. Roos T H et al. *Nucl. Instrum. Meth. Phys. Res. A* **651** 329 (2011)
66. Asadizanjani N et al. ''Rapid non-destructive reverse engineering of printed circuit boards by high resolution X-ray tomography'', http://dx.doi.org/10.13140/RG.2.2.27880.21765
67. ''Associated Particle Imaging (API)'', Report DOE/NV/11718-223 (Santa Barbara, CA: Special Technologies Laboratory, 1998)
68. Chichester D L, Lemchak M, Simpson J D *Nucl. Instrum. Meth. Phys. Res. B* **241** 753 (2005)
69. Wellington T A et al. *Phys. Procedia* **66** 432 (2015)
70. ''Neitronnye generatory'' (''Neutron generators''). Dukhov Automatics Research Institute (VNIIA), Rosatom, http://vniia.ru/production/neitronnie-generatory/neytronnye-generatory.php
71. Van Liew S *Nucl. Instrum. Meth. Phys. Res. A* **784** 417 (2015)